

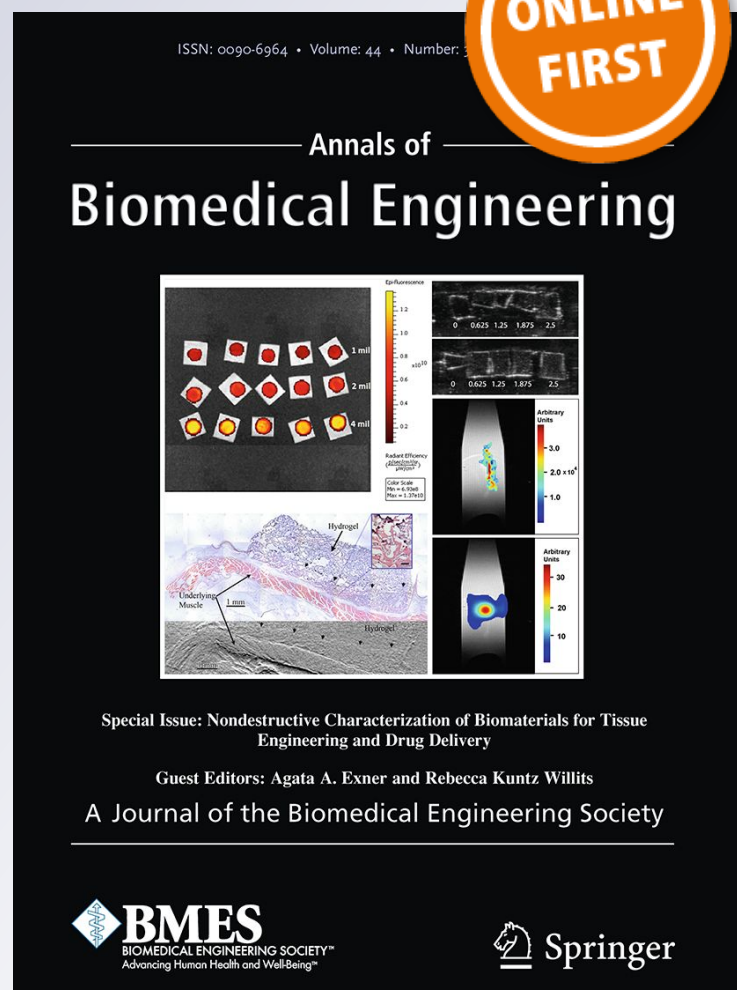
The Contributions of Individual Muscle–Tendon Units to the Plantarflexor Group Force–Length Properties

Mehrdad Javidi, Craig P. McGowan & David C. Lin

Annals of Biomedical Engineering
The Journal of the Biomedical
Engineering Society

ISSN 0090-6964

Ann Biomed Eng
DOI 10.1007/s10439-019-02288-z



Your article is protected by copyright and all rights are held exclusively by Biomedical Engineering Society. This e-offprint is for personal use only and shall not be self-archived in electronic repositories. If you wish to self-archive your article, please use the accepted manuscript version for posting on your own website. You may further deposit the accepted manuscript version in any repository, provided it is only made publicly available 12 months after official publication or later and provided acknowledgement is given to the original source of publication and a link is inserted to the published article on Springer's website. The link must be accompanied by the following text: "The final publication is available at link.springer.com".



The Contributions of Individual Muscle–Tendon Units to the Plantarflexor Group Force–Length Properties

MEHRDAD JAVIDI,¹ CRAIG P. MCGOWAN,^{2,3,4} and DAVID C. LIN^{1,4,5}

¹Voiland School of Chemical Engineering and Bioengineering, Washington State University, PO Box 646515, Pullman, WA 99164-6515, USA; ²Department of Biological Sciences, University of Idaho, 875 Perimeter Drive, MS 3051, Moscow, ID 83844, USA; ³WWAMI Medical Education Program, University of Idaho, 875 Perimeter Drive, MS 4207, Moscow, ID 83844, USA; ⁴Washington Center for Muscle Biology, Washington State University, PO Box 646515, Pullman, WA 99164, USA; and ⁵Department of Integrative Physiology and Neuroscience, Washington State University, PO Box 647620, Pullman, WA 99164, USA

(Received 21 December 2018; accepted 9 May 2019)

Associate Editor Dan Elson oversaw the review of this article.

Abstract—The combined force–length (F–L) properties of a muscle group acting synergistically at a joint are determined by several aspects of the F–L properties of the individual musculotendon units. Namely, misalignment of the optimal lengths of the individual muscles will affect the group F–L properties. This misalignment, which we named M_{opt}^{MT} , arises from the properties of the muscles (i.e., optimum fiber length and pennation angle) and of their tendons (i.e., compliance and slack length). The aim of this study was to measure the F–L properties of kangaroo rat plantarflexors as a group and individually and determine the effects of M_{opt}^{MT} on the group F–L properties. Specifically, we performed a sensitivity analysis to quantify how M_{opt}^{MT} influences the tradeoff between maximizing the peak force vs. having a wider group F–L curve. In the kangaroo rat, we found that the optimal lengths of two bi-articular musculotendon units, the plantaris and the gastrocnemius, were misaligned by 1.8 mm, but this amount favored maximal peak force rather than increasing F–L curve width. Because we measured the misalignment *in situ*, we could directly assess the tradeoff between maximizing peak force vs. a wider F–L curve without making modeling assumptions about the individual muscle or tendon properties.

Keywords—Kangaroo rat, Muscle optimal length, Force–length properties.

ABBREVIATIONS

F Force measured by servomotor (N)
 L^{MT} Musculotendon length equal to distance

Address correspondence to David C. Lin, Voiland School of Chemical Engineering and Bioengineering, Washington State University, PO Box 646515, Pullman, WA 99164-6515, USA. Electronic mail: davidlin@wsu.edu

between origin of muscles and motor arm (mm)
 ΔL^{MT} Change in musculotendon length (mm)
 F^{GRP} Musculotendon force of the muscle group (N)
 F_a^{GRP} Active force of muscle group (N)
 F_p^{GRP} Passive force of muscle group (N)
 F_a^M Active force of muscle M (either gastrocnemius (GAS) or plantaris (PL)) (N)
 F_p^M Passive force of muscle M (N)
 F_o^{GRP} Maximum isometric force of the muscle group (N)
 F_o^M Maximum isometric force of the muscle M (N)
 L_{o-GRP}^{MT} Musculotendon length at maximum isometric force of muscle group (mm)
 L_o^{MT*} Initial musculotendon length, which is an estimation of L_{o-GRP}^{MT} (mm)
 L_{o-M}^{MT} Musculotendon length at maximum isometric force of muscle M (mm)
 L_o^M The length of muscle belly M at maximum isometric force of muscle M (mm)
 L_c^M Distance between the pair of sonometric crystals inserted into muscle M (mm)
 L_{o-c}^M Distance between crystal pair at maximum isometric force of muscle M (mm)
 θ_f^M Pennation angle of muscle M (degrees)
 L_f^M Fiber length of muscle M (mm)
 CSA^M Functional cross sectional area of muscle M (mm^2)
 σ_{max} Maximum isometric stress (kPa)
 L_{s-M}^T Slack length of the tendon of muscle M (mm)

$\varepsilon_{\max-M}^T$	Tendon strain of muscle M at its maximum isometric force ($\%L_{s-M}^T$)
L^{ac}	Relative displacement between the two muscle-tendon units (mm)
M_{opt}^{MT}	Distance between L_{o-M}^{MT} of two different muscles (mm)
F_{max}	Maximum force of the F-L curve of muscle group calculated by model (N)
W	Width of the F-L curve of the muscle group calculated by model (mm)

optimal length (with respect to joint angle) within a group could be experimentally measured.

Kangaroo rats are small bipedal hoppers (mass approximately 100 g) that can jump vertically ten times their standing hip height.²⁵ In kangaroo rats, the three bi-articular plantarflexor muscles include the lateral and medial gastrocnemius (LG and MG, respectively) and plantaris (PL), and they provide the greatest contribution to the moment output at ankle joint.²⁵ The SOL is the only uni-articular plantarflexor, but it is very small in kangaroo rats (about 2% of total plantarflexor mass), so its contribution to the group force is minimal.^{2,3,19} The LG and MG together (the GAS) has a distinct and separate tendon from the PL tendon, and all merge to the same point on the calcaneus.¹⁹ Thus, the mechanical actions of those three muscles are identical in the sagittal plane and can be assumed to sum together. Therefore, kangaroo rat plantarflexors are an excellent model in which to examine the functional significance of optimal length alignment because these muscles are primary contributors to a well-defined locomotor behavior (i.e., jumping).

The objective of this study was to experimentally measure the misalignment of optimal length within a synergistic muscle group and determine the functional significance for that amount of misalignment. To do so, we measured the F-L properties of the plantarflexor muscles as a group (GAS and PL), and then we measured the F-L properties of the GAS when the PL tendon was cut. Modeling was then performed to determine the sensitivity of the group properties (the width and peak isometric force of F-L curve) to a change in the optimal length alignment of the individual muscles. The outcomes of this study have implications for understanding in what way the differences in the optimal lengths of the individual muscles influence the group properties.

INTRODUCTION

The force-length (F-L) properties of a skeletal muscle are functionally important because they determine the maximum isometric force across the range of motion of the muscle. Likewise, the F-L properties will impact the maximum moment that can be generated across the range of motion of a joint. However, in many joints, the moment-angle properties arise from multiple synergistic muscles, and the F-L properties of each individual muscle relative to those of the other synergist(s) acting at the joint could be different. Specifically, the optimal lengths of the individual muscle F-L curves may not occur at the same length (i.e., misalign) determined by the angle of the joint spanned by the muscles. The amount of optimal length misalignment will influence the tradeoff of two aspects of the moment-angle properties: the peak moment of the moment-angle relationship, such that no misalignment will result in the largest peak moment possible; and the width of the moment-angle relationship, such that more misalignment will result in a broader curve because the individual muscles would be operating on different portions of their F-L curve for the same joint angle. Assessing this tradeoff will elucidate how the properties of individual muscles combine to determine the moment generation of a synergistic muscle group.

Different approaches have been used to examine this tradeoff, particularly in human ankle plantarflexors. Musculoskeletal models combined with optimization methods and imaging can explain how individual muscles contribute to *in vivo* moment measurements.^{6,7,24} However, uncertainty in the results can arise from a number of assumptions. For example, tendon slack length is a model parameter that is difficult to estimate, sets each muscle's optimal length with respect to the joint angle, and strongly influences the modeling results.^{1,5,26,30} Thus, examination of the tradeoff between maximizing peak moment and having wider moment-angle curve is better addressed in an animal model because each muscle's F-L curve and

MATERIALS AND METHODS

Animals

All experimental procedures completed were approved by the Institutional Animal Care and Use Committee (IACUC) at Washington State University. Experiments were performed with 6 adult kangaroo rats (*Dipodomys deserti*) (3 males, 3 females, average mass \pm SD = 100.4 \pm 23.6 g, ages unknown). The animals were wild caught in the Mojave Desert near Gold Butte, Nevada using extra-long Sherman traps. All trapping was done under permits from the Nevada Department of Wildlife and the Bureau of Land Management following procedures approved by the University of Idaho Animal Care and Use Committee.

Surgical Procedure

Animals were initially anesthetized for 3 min inside a plastic enclosure with isoflurane (3%) for handling purposes. Animals were then placed under a mask with 1% isoflurane flow until paw withdraw was negative. Subsequently, animals were deeply anesthetized with an intraperitoneal injection of 50 mg/kg Ketamine and 0.15 mg/kg Dexmedetomidine and isoflurane rate was decreased to 0.5% for the duration of the experiment. During surgery, animals were placed on a temperature-controlled surgery pad (37 °C). The plantarflexor muscles of the right leg with their tendons were dissected from surrounding muscles and tissues, leaving the proximal end attached to the femur, major blood vessels intact, and the distal tendons attached to the calcaneus, which was later cut to create a bone chip attached to the tendon. To prevent dehydration, exposed muscles were regularly irrigated with Ringer's solution. The sciatic nerve was cut proximally. Distally, the tibial branch was left intact and the other branches were cut. To sonometrically measure the muscle belly length changes of the LG, MG, and PL, a pair of piezoelectric crystals (1.0 mm diameter; Sonometrics Corp) was implanted near the proximal and distal aponeurosis of each muscle (see Fig. 1, white circles on LG as an example). Due the small size of SOL (see “Introduction”), it was not possible to insert crystals into the muscle, so the muscle and its tendon were carefully removed.

Experimental Setup

Kangaroo rats were placed prone on a horizontal heating platform (1300A; Aurora Scientific, Aurora,

ON, Canada) which was modified to accommodate the size of a kangaroo rat (Fig. 1). A servomotor (309C; Aurora Scientific, Aurora, ON, Canada) measured both force and position while operating in the length control mode for isometric contractions.

To mechanically ground the origin of the muscle group, a stainless steel intramedullary pin (0.7 mm O.D.) was inserted distally through the femur, exiting percutaneously on the proximal end. Both exposed ends of the pin were secured to a custom-fabricated support arm, which was then attached to the platform. Because of the large forces which can be generated by kangaroo rat muscles, a wire (0.5 mm O.D.) was looped around the middle of the femur and support arm to prevent any horizontal displacements of the femur. The exposed muscle group was immersed in a custom-made temperature-controlled (37 °C) trough of mineral oil for the duration of testing to prevent muscle dehydration and maintain temperature. The calcaneal bone chip was then attached to the lever-arm of the servomotor (Fig. 1) and the sciatic nerve was placed onto bipolar hook electrodes (0.3 mm silver wire). A rectal temperature probe and pulse oximeter (PhysioSuite; Kent Scientific, Torrington, CT) placed on the paw allowed for continuous monitoring of core body temperature, oxygenation level, and heart rate.

Experimental Protocols

Servomotor force (equivalent to musculotendon (MT) force, F), servomotor arm position (equivalent to the change in MT length, ΔL^{MT}), and distances between the pairs of sonometric crystals inserted into individual muscles (L_c^M) (Fig. 1) were recorded at

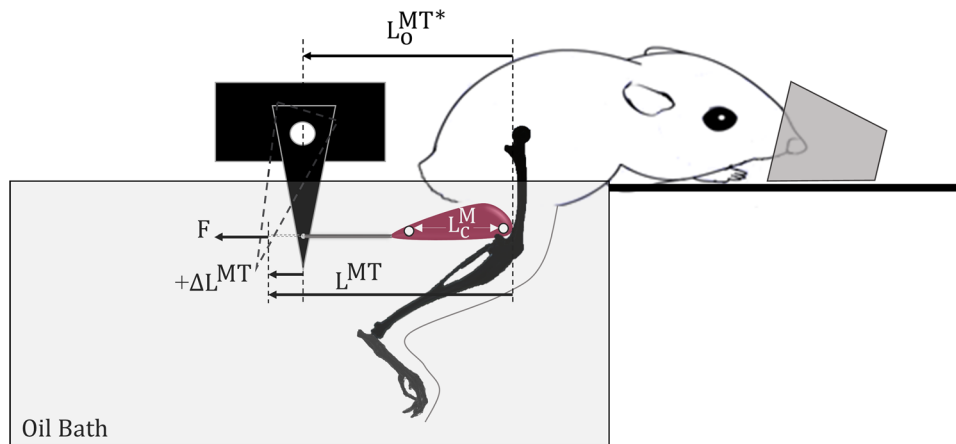


FIGURE 1. Schematic of the experimental setup. F , L_o^{MT*} , ΔL^{MT} and L_c^M were measured force, fixed position of the motor with respect to origin of muscle group, which was set to the initial estimate of optimum length of the muscle group (see experimental protocol (i)), change in the horizontal position of the motor arm with respect to its position when vertical, which was equal to the change in the group muscle–tendon (MT) length, and distance between the sonometric crystal pair, respectively. L^{MT} was the group muscle–tendon length calculated by: $L^{MT} = L_o^{MT*} \pm \Delta L^{MT}$.

1000 Hz (Real-Time Muscle Data Acquisition, Aurora Scientific, Aurora, ON, Canada). A sequence of three protocols was followed (details found below): (i) initial MT length and stimulation amplitude were set; (ii) isometric contractions of the muscle group (GRP); and (iii) isometric contractions of GAS (MG and LG together) after cutting the PL tendon. It is important to note that, in kangaroo rats, it is not possible to separate the LG and MG muscles or their tendons without damaging them, so we had to consider the two muscles as a single entity (see “[Discussion](#)”).

To set the initial MT length, we followed a protocol similar to a previous study in dystrophic mice.²¹ Briefly, after preconditioning with sinusoidal movements and low-level stimulation, the servomotor arm was held in place while the relaxed muscle group was stretched by changing the motor position until passive force was 150 to 200 mN. From preliminary experiments, this range of passive force roughly corresponded to the optimal length of the muscle group (L_{o-GRP}^{MT}) and relates to the observation that passive force is nonzero around optimal length.²⁰ For the remainder of the experiment, motor position was not changed and only the servomotor arm was used to change MT length. We defined this MT length as L_o^{MT*} (i.e., the estimate of the length which is L_{o-GRP}^{MT}) (Fig. 1). We then evaluated the twitch responses of five increasing stimulation amplitudes (0.5, 1, 1.5, 2, and 2.5 mA) of 0.2 ms biphasic pulses. The minimum amplitude to produce maximal twitch response was identified and 150% of this value was defined as the supramaximal stimulation amplitude and used for all the following tetanic stimulations.

The isometric force of the muscle group was measured at a minimum of seven different MT lengths within a range of $L^{MT} = L_o^{MT*} + \Delta L^{MT}$, where $-4 \leq \Delta L^{MT} \leq +3$ mm, and by generating supramaximal tetanic contractions with 300 ms trains of 0.2 ms biphasic pulses at 150 Hz. To prevent fatigue, muscles were rested for 3 min following each tetanus. After plotting the active muscle group force-MT length curve (see “[Data Analysis](#)”), if there were no measurements on the descending limb (i.e., longer lengths producing smaller forces), additional measurements were obtained at longer lengths.

After cutting the PL tendon at the proximal end near the junction of the PL muscle and tendon, isometric contractions similar to protocol (ii) were performed on GAS muscles to obtain its F–L relationship (see “[Data Analysis](#)”). To minimize force transmission from PL to GAS after cutting the PL tendon, which can occur *via* surrounding connective tissue,^{13,22} we removed the surrounding tissue as much as possible. This also let the PL muscle shorten to its slack length, when it can only generate a minimal amount of force.

Anatomical Measurements

After euthanasia and dissecting the muscle from their tendon, the mass of each muscle (M) was measured. Functional cross-sectional area (CSA) was then calculated by¹⁷:

$$CSA^M = (m \times \cos(\theta_f^M)) / (L_f^M \times \rho) \quad (1)$$

where ρ is the density of mammalian muscle of 1.06 mg/mm³,¹⁵ L_f^M is fiber length and θ_f^M is the pennation angle of the muscles. To measure the CSA of individual muscles, we used the mean fiber lengths ($L_f^{PL} = 8.8$, $L_f^{LG} = 16.0$ and $L_f^{MG} = 13.7$ mm) and mean pennation angles ($\theta_f^{PL} = 22.8$, $\theta_f^{LG} = 18.8$ and $\theta_f^{MG} = 22.6$ deg) measured previously by our lab from a large sample of kangaroo rats with the same weight range.¹⁹ The fiber lengths calculated in this study were the estimations of optimum fiber lengths.

Data Analysis

For each trial, total force was found by averaging the force recording from 150 to 250 ms after initial stimulation (on the plateau of each tetanus). Active force was calculated as the difference between total force and initial passive force. Thus, for each animal, force-MT length relationships of the GRP, GAS and PL were defined as follows:

$$F_a^{GRP}(L^{MT}) = F_t^{GRP}(L^{MT}) - F_p^{GRP}(L^{MT}) \quad (2)$$

$$F_a^{GAS}(L^{MT}) = F_t^{GAS}(L^{MT}) - F_p^{GAS}(L^{MT}) \quad (3)$$

$$\begin{aligned} F_a^{PL}(L^{MT}) &= F_a^{GRP}(L^{MT}) \\ &- F_a^{GAS}(L^{MT}) = (F_t^{GRP}(L^{MT}) - F_t^{GAS}(L^{MT})) \\ &- (F_p^{GRP}(L^{MT}) - F_p^{GAS}(L^{MT})) \end{aligned} \quad (4)$$

where the a, p, and t subscripts represent the active, passive, and total forces for the muscles denoted by the superscripts of GRP, GAS, and PL. The active F–L relationships for GRP and GAS were fitted to 3rd order polynomial functions (constrained to assure a single peak/inflection point) from the active forces and L^{MT} data measured during protocols (ii) and (iii) using custom software written in MATLAB (MathWorks, Natick, MA). For the PL F–L relationship, we assumed that the PL force was the difference between GRP and GAS force (Eq. 4). The passive F–L relationships were estimated by fitting to exponential functions ($F_p(L^{MT}) = c_1 e^{(c_2 L^{MT})}$) for data measured during protocols (ii) and (iii), respectively.

We wanted to obtain the F–L curves of the group, GAS, and PL normalized to maximal force and opti-

mal MT length of each muscle. From the peak of the polynomial fitted active force–MT length curve of each animal, maximal tetanic force of the muscle group (F_o^{GRP}), GAS (F_o^{GAS}) and PL (F_o^{PL}) and the optimum MT length of muscle group (L_o^{MT-GRP}), GAS (L_o^{MT-GAS}) and PL (L_o^{MT-PL}) were estimated. Specific tensions (STs) were calculated as the maximum of measured muscle force (at the tendon) divided by functional cross sectional area ($\sigma_{max} = F_o/CSA$). The active and passive forces of GRP, GAS and PL from each animal were normalized by its maximum isometric force (F_o) and the L^{MT} was converted to the length with respect to its optimum length (L_o^{MT}). To obtain a F–L curve representing all normalized forces and referenced MT lengths from the 6 animals, data were pooled and fitted to a 3rd order polynomial function.

To find the muscle belly lengths of individual muscles during isometric contractions of the muscle group, sonometric data were used to obtain the normalized force and muscle belly length relationships of the GAS and PL. At each L^{MT} , the forces generated by GAS and PL were known from Eqs. (2) and (3) and the crystal distances in individual muscles were used to obtain muscle belly length normalized to the optimum muscle belly length. To do so, for each animal, active force (F_a) and crystal distance (L_c) data from GAS and PL were fitted to a 3rd order polynomial function. Maximum isometric force (F_o) of individual muscles was measured as the peak value, along with its associated (optimal) crystal distance (L_{o-c}). Then, for each animal, forces and crystal distances were normalized by F_o and L_{o-c} , respectively. At this step, because of the similarity between the normalized crystals distance of L_c^{LG} and L_c^{MG} (average difference between normalized crystal distances was 0.02 ± 0.002), the average of those values were considered as normalized L_c^{GAS} . We assumed that amount of strain in crystal distance was equal to the amount of strain in the whole muscle belly, so the crystal distances (L_c) normalized by optimum crystal distance (L_{o-c}) will be equal to the muscle belly length (L_M) normalized by optimum muscle belly length (L_{o-M}). Finally, all normalized forces and muscle belly lengths from all animals were pooled and fitted to 3rd order polynomial functions to obtain the normalized F–L relationships of individual muscles.

To estimate the contribution of GAS and PL muscles to the group force at different L^{MT} , we normalized F_a^{GRP} , F_a^{GAS} and F_a^{PL} by F_o^{GRP} and referenced L^{MT} by L_o^{MT-GRP} . These F–L curves for the GAS and PL of all animals were pooled and fitted to 3rd order polynomial functions.

Sensitivity Analysis

A sensitivity analysis was performed to predict the effects of individual MT properties on the muscle group force–MT length relationship. The parameter M_{opt}^{MT} was defined as the misalignment between optimum MT lengths of individual muscle–tendon units ($M_{opt}^{MT} = L_o^{MT-GAS} - L_o^{MT-PL}$). In general, for two different MT units, the parameter M_{opt}^{MT} is related to the F–L properties of the muscles, tendon properties and the relative displacement of muscle–tendon units (which can arise from one muscle being uni-articular and the other bi-articular). The relationship between parameter M_{opt}^{MT} and properties mentioned above are derived in Supplementary material A and can be expressed as:

$$M_{opt}^{MT} = (L_o^A - L_o^B) + ((1 + \epsilon_{max-A}^T)L_{s-A}^T(1 + \epsilon_{max-B}^T)L_{s-B}^T) - L^{ac} \quad (5)$$

where A and B represent two different muscles (Fig. 2). L_s^T and ϵ_{max}^T are the tendon slack length and tendon strain at maximum isometric force, respectively. L^{ac} is the relative displacement between muscle–tendon units of A and B at maximum isometric force of the group which is equal to zero in our experiments because all muscle–tendon unit lengths were constrained identically. To elucidate the consequences of changes in M_{opt}^{MT} for the group F–L properties, we measured the sensitivity of the maximum force (F_{max}) and the width (W) of $F^{GRP} L^{MT}$ relationship to the parameter M_{opt}^{MT} . W was defined as the width of the group force–MT length at 80% of F_{max} (ascending to descending limb).

Statistics

Two-sided sign test was performed using the MATLAB statistical toolbox to test the hypothesis that the optimum MT lengths of individual muscles relative to the group ($L_o^{MT-GRP} - L_o^{MT-M}$) has a distribution with zero median (aligned) against the alternative that the distribution does not have zero median (not aligned). The sign test was used instead of a paired t test because of the small sample size ($n = 6$). Significance was set at confidence level of $\alpha = 0.05$.

RESULTS

Anatomical Measurements

All results are presented as mean \pm standard deviation (SD) from six animals. The masses of the PL, LG and MG muscles were 0.34 ± 0.11 , 0.47 ± 0.11 and 0.47 ± 0.14 g, respectively. The calculated CSA of PL,

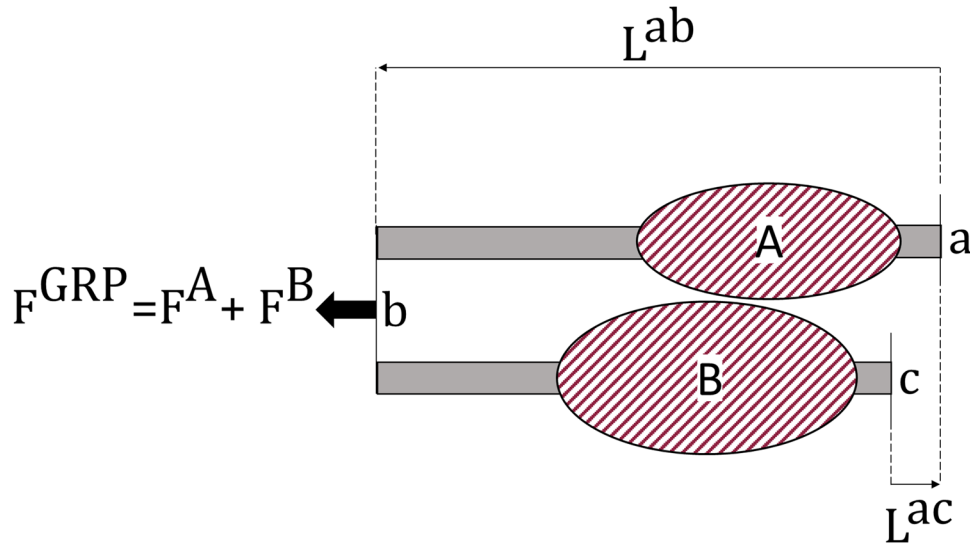


FIGURE 2. The general schematic of two different muscle–tendon units. In our study, muscles A and B were the GAS and PL, respectively. Points a and c were attached to the same point of femur, thus L^{ac} was zero. Point b was attached to the motor arm.

LG and MG muscles were 33.75 ± 10.73 , 26.26 ± 5.91 and $30.06 \pm 8.66 \text{ mm}^2$, respectively.

Properties of Individual Muscle–Tendon Units and the Group

The relationships between normalized force and L^{MT} for the muscle group, GAS and PL all showed clear peaks and ascending and descending limbs (Fig. 3). The maximum isometric forces of muscle group, GAS and PL were $F_o^{GRP} = 25.3 \pm 6.4$, $F_o^{GAS} = 18.1 \pm 4.8$ and $F_o^{PL} = 8.4 \pm 2.8 \text{ N}$, respectively. CSA of the muscle group was estimated as the summation of the CSA of all muscles and for GAS it was equal to the summation of the CSA of LG and MG. The STs were $\sigma_{max}^{GRP} = 286 \pm 41$, $\sigma_{max}^{GAS} = 322 \pm 37$ and $\sigma_{max}^{PL} = 258 \pm 89 \text{ kPa}$. To estimate the contribution of LG and MG muscles to GAS force, we assumed that STs of the LG and MG were equal to that of the GAS ($\sigma_{max}^{LG} = \sigma_{max}^{MG} = \sigma_{max}^{GAS}$) and the force was proportional to their CSA. The resulting estimated maximum isometric forces were $F_o^{LG} = 8.4 \pm 1.7$ and $F_o^{MG} = 9.7 \pm 3.2 \text{ N}$. Normalized F–L properties of the individual muscles, plotted as a function of muscle length, were derived from the sonometric data (Fig. 4).

Force Contributions of Individual Muscle–Tendon Units to the Group

Contributions of the PL and GAS to the group force were calculated as a function of L^{MT} relative to L_{o-GRP}^{MT} (Fig. 5a). The maximum isometric force of PL (F_o^{PL}) and GAS (F_o^{GAS}) were 34 ± 8 and 71 ± 10 per-

cent of the maximum isometric force of muscle group (F_o^{GRP}). The peaks of PL and GAS were at the lengths that did not align with the optimum MT length of the group (L_{o-GRP}^{MT}). The optimum MT length of GAS and PL with respect to the L_{o-GRP}^{MT} were $0.5 \pm 0.3 \text{ mm}$ ($p = 0.03$) and $-1.3 \pm 0.4 \text{ mm}$ ($p = 0.03$), respectively (Fig. 5a). Because of the discrepancy in optimal lengths, at the optimum length of muscle group, GAS and PL produced force equal to 99 and 89% of their maximum isometric force, respectively. Based upon their muscle F–L curves (Fig. 4), this result implies that the GAS and PL were at 99% and 104% of their optimum length when they were activated together as a group to generate the maximum GRP force, respectively.

Sensitivity Analysis

We performed a sensitivity analysis for the effects of shifting the optimal lengths of the GAS and PL on two metrics of the group FL curve: $F_{max} (\% F_o^{GRP})$ and W (Fig. 5a). We defined a parameter, M_{opt}^{MT} , as the misalignment between the L_{o-GAS}^{MT} and L_{o-PL}^{MT} . In the kangaroo rat plantarflexors, M_{opt}^{MT} was experimentally measured to be 1.8 mm. Amounts of change in F_{max} and W of the F–L properties of the group relative to their experimentally measured values were calculated at 9 different values of M_{opt}^{MT} (Fig. 5b). Sensitivity analyses indicated that the maximum isometric force of the plantarflexors of the kangaroo rat cannot be larger than $1.05 F_o^{GRP}$ for $M_{opt}^{MT} = 0$ when $F_{max} = F_o^{PL} + F_o^{GAS}$ and cannot be lower than $0.71 F_o^{GRP}$ for

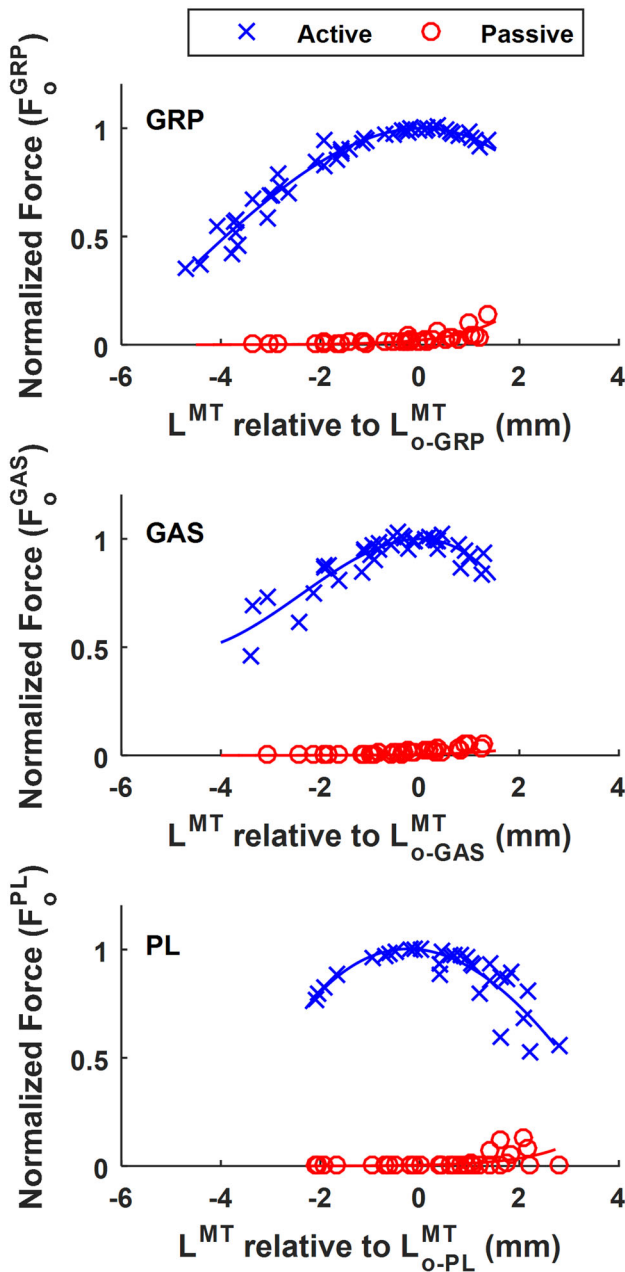


FIGURE 3. Normalized force and converted MT length relationships of the muscle group (GRP), GAS and PL for all animals ($n = 6$). The active and passive forces of the GRP, GAS and PL were normalized by the maximum isometric forces of GRP (F_o^{GRP}), GAS (F_o^{GAS}) and PL (F_o^{PL}), respectively. Converted MT length of GRP, GAS and PL were the musculotendon lengths (L^{MT}) relative to the musculotendon lengths associated with maximum isometric force of GRP (L_{o-GRP}^{MT}), GAS (L_{o-GAS}^{MT}) and PL (L_{o-PL}^{MT}). The fitted curves to the normalized force (active, passive) and converted MT length of GRP ($R^2 = 0.965$, $R^2 = 0.707$), GAS ($R^2 = 0.837$, $R^2 = 0.845$) and PL ($R^2 = 0.728$, $R^2 = 0.190$) are also indicated.

$M_{opt}^{MT} = 5.3$ mm when further misalignment does not change the peak combined force (such that $F_{max} = F_o^{GAS}$ because the descending limb of the PL

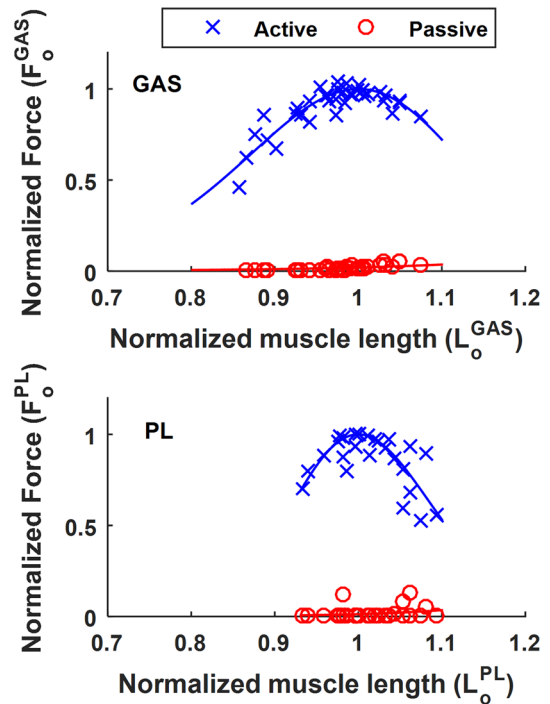


FIGURE 4. Normalized force–length curve of GAS and PL for all animals ($n = 6$). Active and passive forces of GAS and PL were normalized by the maximum isometric force of GAS (F_o^{GAS}) and PL (F_o^{PL}), respectively. Muscle belly lengths of GAS and PL were normalized by the optimum muscle belly length of GAS (L_o^{GAS}) and PL (L_o^{PL}), respectively. The fitted curves to the normalized force (active, passive) and normalized muscle belly length of GAS ($R^2 = 0.800$, $R^2 = 0.481$) and PL ($R^2 = 0.507$, $R^2 = 0.486$) are also indicated.

no longer overlaps with the optimal length of the GAS) (Fig. 5b). Notably, M_{opt}^{MT} changes in F_{max} and W were nonlinear. For example, for $0 \leq M_{opt}^{MT} \leq 2.7$ mm, the F–L properties of the group stayed approximately constant, while for $2.7 \leq M_{opt}^{MT} \leq 5$ mm, the changes in the group F–L properties were more substantial. This implies that the effects of aligning the optimum lengths of individual muscle–tendon units (i.e., decreasing M_{opt}^{MT}) on the muscle group properties were smaller than separating them (i.e., increasing M_{opt}^{MT}).

DISCUSSION

The aim of this study was to measure the F–L properties of kangaroo rat plantarflexors as a group and individually and determine the effects of optimal length misalignment on the group F–L properties (width and maximum force). The combination of measurements with sensitivity analyses provides a better understanding of how the properties of individual muscles can be combined to create a spectrum of mechanical behavior, within which the group

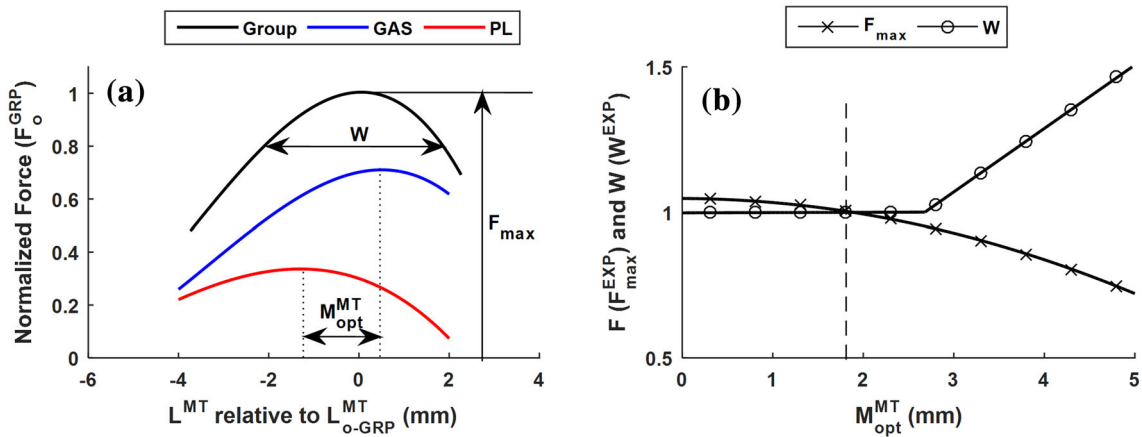


FIGURE 5. (a) The contribution of individual muscles to muscle group force. M_{opt}^{MT} is the distance between L_{o-GAS}^{MT} and L_{o-PL}^{MT} . Forces of individual muscles are normalized by the maximum isometric force of the muscle group. F_{max} and W are the maximum force produces by muscle group and width of the muscle group force-MT length curve at 80% of F_{max} , respectively. (b) The sensitivity of F_{max} and W , relative to their experimentally measured values, to changes in M_{opt}^{MT} . Vertical dashed line shows the experimental value of M_{opt}^{MT} and on the right (left) side of the line misalignment increased (decreased).

properties can be tailored to match the desired motor function.

Functional Relevance of the Measured Properties of Individual Muscles and the Group

In earlier studies of jumping by kangaroo rats, the ST of GAS, PL and SOL muscles, together, was estimated from electrical stimulation of the muscles as 200 kPa.^{2,3} However, there was an uncertainty about this value because of methodological constraints and a large difference between the ST and the maximum stress estimated from inverse dynamics during the jumps ($ST_{highest\ jump} = 1.75 ST_{stimulated}$). Our estimates of $\sigma_{max}^{GAS} = 322 \pm 15$, $\sigma_{max}^{PL} = 258 \pm 37$, and $\sigma_{max}^{GRP} = 286 \pm 17$ kPa agree better with the values estimated during the jumps. Comparatively, the STs from *in situ* experiments on the SOL, PL and GAS of several species, such as mouse, rat, rabbit, cat and hopping mouse, were measured in the range from 150 to 250 kPa (with a couple of exceptions).²³ This range is less than the STs of kangaroo rat plantarflexors, either individually or as a group. Therefore, the data obtained here suggest that k-rats have comparatively stronger plantarflexor muscles, which may be necessary to accomplish their extreme jumping performance.

We found that one of the key differences in the F–L properties between muscles was the misalignment of optimal lengths. This is consistent with a recent study which reported the differences between optimum lengths of GAS and PL of Wistar rat muscles relative to the group optimal length were + 0.4 and – 1.2 mm.¹⁶ Interestingly, these values were very similar to + 0.5 and – 1.3 mm which we measured for

GAS and PL of the kangaroo rat, respectively. This misalignment changes the relative force contribution of an individual muscle to the group force as the musculotendon length changes. For example, the relative force contribution of the GAS is at its largest when the musculotendon length is near the optimal length of the GAS (Fig. 5a). In fact, the relative contribution of an individual muscle to the group force throughout the entire musculotendon length range cannot be constant whenever there is optimal length misalignment between two muscles. The assumption of a constant relative contribution of a muscle across the range of motion is often made in human studies (see Ref. 8 for review) but should be reconsidered in light of the results presented here.

To assess the functional effects of the measured misalignment, we performed a sensitivity analysis by manipulating the misalignment (M_{opt}^{MT}) and determining the effects on the tradeoff between F_{max} and W (Fig. 5). The results of our sensitivity analysis indicated that M_{opt}^{MT} is within the range of values (Fig. 5b) where maximal group force is close to its largest possible value. Therefore, the plantarflexors of the kangaroo rat function synergistically to generate maximal force to power its jumps, in contrast to being tuned as a group to generate forces over a wide range of motion.

Study Limitations

An assumption that we used for measurement of the properties of the individual plantarflexors was that F–L properties of PL were equal to the F–L curve of the group (PL + GAS) minus the F–L curve of GAS. This assumption has two presumptions. First, after

cutting the PL tendon, the PL cannot transmit force to the GAS. We attempted to minimize inter-muscular force transmission, shown to occur in the plantarflexors of rats,^{14,27–29} by freeing the PL from the surrounding tissue as much as possible (see Methods), and the effectiveness of this procedure was confirmed by the PL shortening to a slack length. However, force transmission might have still occurred, potentially reflected by the specific tension of the GAS being larger than that of the PL. The second presumption is that the force generated by the PL does not influence the length of the GAS through a common tendon. In other words, PL force induces stretch of a tendon that is also attached to the GAS, thus the GAS is shorter for a given musculotendon length (than when the PL force is reduced). In the kangaroo rat, this scenario does not occur due to the complete separation of the PL and GAS tendons (see “Materials and Methods”). In other species, the tendons of the PL and GAS cannot be assumed to have no interactions.²⁹

In the experimental protocols, we did not include the additional plantarflexors: flexor hallucis longus (FHL), flexor digitorum longus (FDL), and soleus. In kangaroo rats, the FHL and FDL provide little plantarflexor moment due to their very small moment arms¹⁹ and the soleus is very small (see “Materials and Methods”). Thus, these muscles are not functionally important to generating plantarflexor moment during behaviors such as jumping. In addition, removing these muscles clarified the effects of optimal length misalignment in the two muscles considered, the GAS and PL. However, in other species, the contribution of the soleus, due to its relative size, cannot be neglected in considering how the F–L properties of the individual plantarflexors affect the moment–angle properties of the ankle.²⁷

Implications of Misalignment Between Plantarflexors

The shape and optimal length of the F–L curve of a musculotendon unit is influenced by anatomical parameters, such as fiber length and pennation angle, and tendon parameters, such as slack length and stiffness. Thus, misalignment of optimal lengths between two musculotendon units is difficult to accurately model. One of the advantages of an animal model like the kangaroo rat is direct measurement of M_{opt}^{MT} rather than relying on modeling assumptions with its associated uncertainty. For example, tendon slack length is difficult to measure but has one of the largest effects on muscle force predictions from musculoskeletal models.^{1,5,26,30} This is because changing tendon slack length alters where a muscle operates on its F–L curve, affecting the joint angle where peak force is generated and changing the joint range over

which a muscle can generate force.⁹ Thus, if in the process of developing a musculoskeletal model, the assumed slack lengths produce a substantial misalignment between muscle optimal lengths, there will be an effect on the maximal moment that can be generated at the joint which the muscles cross.

Anatomical and tendon parameters are not the only causes of optimal length misalignment. If one of the muscles in the group is uni-articular and another is bi-articular, motion of the joint not spanned by the uni-articular muscle causes a length change in the bi-articular muscle only,¹¹ thus changing the lengths of each musculotendon unit relative to each other. This effect is captured in Fig. 2 and Eq. (5), where the parameter L^{ac} changes due to motion of the joint not spanned by the uni-articular muscle.

In humans, the bi-articular MG and uni-articular SOL are the two plantarflexors with the largest CSAs. To parallel the analysis completed in this study, the MG is represented as the muscle A and SOL as muscle B in Fig. 2. L^{ac} would represent the distance between the proximal ends of SOL and MG, which is defined in the Fig. 2 and Eq. (5) to be a positive value because the SOL musculotendon unit is shorter than that of the MG in humans. In addition, experimental and modeling studies of human plantarflexors support that $L_o^{MG} > L_o^{SOL}$ and $L_{s-MG}^T > L_{s-SOL}^T$ (for example, the muscle and tendon properties reported in here¹⁸). Thus, from Eq. (5), misalignment (M_{opt}^{MT}) for these two specific human plantarflexor muscles must be a positive value which decreases by knee extension. Human experimental studies show maximum plantarflexor moments occurs at full knee extension.^{4,10–12} This observation implies that the optimum length misalignment (M_{opt}^{MT}) between the MG and SOL is at a minimum at full knee extension and increases with knee flexion. Although this hypothesis for human plantarflexors cannot be confirmed experimentally, it could be considered in developing musculoskeletal models of the human ankle.

ELECTRONIC SUPPLEMENTARY MATERIAL

The online version of this article (<https://doi.org/10.1007/s10439-019-02288-z>) contains supplementary material, which is available to authorized users.

ACKNOWLEDGMENTS

Work supported by Army Research Office #66554-EG (DCL and CPM) and National Science Foundation #1553550 (CPM).

REFERENCES

- ¹Ackland, D. C., Y. C. Lin, and M. G. Pandy. Sensitivity of model predictions of muscle function to changes in moment arms and muscle-tendon properties: a Monte-Carlo analysis. *J. Biomech.* 45:1463–1471, 2012.
- ²Biewener, A. A., and R. Blickhan. Kangaroo rat locomotion: design for elastic energy storage or acceleration? *J. Exp. Biol.* 140:243–255, 1988.
- ³Biewener, A. A., R. Blickhan, A. K. Perry, N. C. Heglund, and C. R. Taylor. Muscle forces during locomotion in kangaroo rats: force platform and tendon buckle measurements compared. *J. Exp. Biol.* 137:191–205, 1988.
- ⁴Dalton, B. H., M. D. Allen, G. A. Power, A. A. Vandervoort, and C. L. Rice. The effect of knee joint angle on plantar flexor power in young and old men. *Exp. Gerontol.* 52:70–76, 2014.
- ⁵De Groot, F., A. Van Campen, I. Jonkers, and J. De Schutter. Sensitivity of dynamic simulations of gait and dynamometer experiments to hill muscle model parameters of knee flexors and extensors. *J. Biomech.* 43:1876–1883, 2010.
- ⁶Fukashiro, S., M. Rob, Y. Ichinose, Y. Kawakami, and T. Fukunaga. Ultrasonography gives directly but noninvasively elastic characteristic of human tendon in vivo. *Eur. J. Appl. Physiol. Occup. Physiol.* 71:555–557, 1995.
- ⁷Hasson, C. J., and G. E. Caldwell. Effects of age on mechanical properties of dorsiflexor and plantarflexor muscles. *Ann. Biomed. Eng.* 40:1088–1101, 2012.
- ⁸Herzog, W. Skeletal muscle mechanics: questions, problems and possible solutions. *J. Neuroeng. Rehabil.* 14:1–17, 2017.
- ⁹Hicks, J. L., T. K. Uchida, A. Seth, A. Rajagopal, and S. L. Delp. Is my model good enough? Best practices for verification and validation of musculoskeletal models and simulations of movement. *J. Biomech. Eng.* 137:020905, 2015.
- ¹⁰Kawakami, Y., Y. Ichinose, and T. Fukunaga. Architectural and functional features of human triceps surae muscles during contraction. *J. Appl. Physiol.* 85:398–404, 1998.
- ¹¹Landin, D., M. Thompson, and M. Reid. Knee and Ankle joint angles influence the plantarflexion torque of the gastrocnemius. *J. Clin. Med. Res.* 7:602–606, 2015.
- ¹²Lauber, B., G. A. Lichtwark, and A. G. Cresswell. Reciprocal activation of gastrocnemius and soleus motor units is associated with fascicle length change during knee flexion. *Physiol. Rep.* 2:e12044, 2014.
- ¹³Maas, H., G. C. Baan, and P. A. Huijting. Muscle force is determined also by muscle relative position: isolated effects. *J. Biomech.* 37:99–110, 2004.
- ¹⁴Maas, H., and T. G. Sandercock. Force transmission between synergistic skeletal muscles through connective tissue linkages. *J. Biomed. Biotechnol.* 1–9:2010, 2010.
- ¹⁵Mendez, J., and A. Keys. Density and composition of mammalian muscle. *Metabolism* 9:184–188, 1960.
- ¹⁶Olesen, A. T., B. R. Jensen, T. L. Uhlendorf, R. W. Cohen, G. C. Baan, and H. Maas. Muscle-specific changes in length-force characteristics of the calf muscles in the spastic Han-Wistar rat. *J. Appl. Physiol.* 117:989–997, 2014.
- ¹⁷Powell, P. L., R. R. Roy, P. Kanim, M. A. Bello, and V. R. Edgerton. Predictability of skeletal muscle tension from architectural determinations in guinea pig hindlimbs. *J. Appl. Physiol.* 57:1715–1721, 1984.
- ¹⁸Rajagopal, A., C. L. Dembia, M. S. DeMers, D. D. Delp, J. L. Hicks, and S. L. Delp. Full-body musculoskeletal model for muscle-driven simulation of human gait. *IEEE Trans. Biomed. Eng.* 63:2068–2079, 2016.
- ¹⁹Rankin, J. W., K. M. Doney, and C. P. McGowan. Functional capacity of kangaroo rat hindlimbs: adaptations for locomotor performance. *J. R. Soc. Interface* 15:20180303, 2018.
- ²⁰Rassier, D. E., B. R. MacIntosh, and W. Herzog. Length dependence of active force production in skeletal muscle. *J. Appl. Physiol.* 86:1445–1457, 1999.
- ²¹Rehwaltdt, J. D., B. D. Rodgers, and D. C. Lin. Skeletal muscle contractile properties in a novel murine model for limb girdle muscular dystrophy 2i. *J. Appl. Physiol.* 123:1698–1707, 2017.
- ²²Rijkelijkhuisen, J. M., G. C. Baan, A. de Haan, C. J. de Ruiter, and P. A. Huijting. Extramuscular myofascial force transmission for in situ rat medial gastrocnemius and plantaris muscles in progressive stages of dissection. *J. Exp. Biol.* 208:129–140, 2005.
- ²³Rospars, J. P., and N. Meyer-Vernet. Force per cross-sectional area from molecules to muscles: a general property of biological motors. *R. Soc. Open Sci.* 3:160313, 2016.
- ²⁴Rugg, S. G., R. J. Gregor, B. R. Mandelbaum, and L. Chiu. In vivo moment arm calculations at the ankle using magnetic resonance imaging (MRI). *J. Biomech.* 23:495–501, 1990.
- ²⁵Schwaner, M. J., D. C. Lin, and C. P. McGowan. Jumping mechanics of desert kangaroo rats. *J. Exp. Biol.* 221:jeb186700, 2018.
- ²⁶Scovill, C. Y., and J. L. Ronsky. Sensitivity of a Hill-based muscle model to perturbations in model parameters. *J. Biomech.* 39:2055–2063, 2006.
- ²⁷Tijs, C., J. H. Van Dieën, G. C. Baan, and H. Maas. Three-dimensional ankle moments and nonlinear summation of rat triceps surae muscles. *PLoS ONE* 9:e111595, 2014.
- ²⁸Tijs, C., J. H. van Dieën, G. C. Baan, and H. Maas. Synergistic co-activation increases the extent of mechanical interaction between rat ankle plantar-flexors. *Front. Physiol.* 7:1–8, 2016.
- ²⁹Tijs, C., J. H. van Dieën, and H. Maas. No functionally relevant mechanical effects of epimuscular myofascial connections between rat ankle plantar flexors. *J. Exp. Biol.* 218:2935–2941, 2015.
- ³⁰Xiao, M., and J. Higginson. Sensitivity of estimated muscle force in forward simulation of normal walking. *J. Appl. Biomech.* 26:142–149, 2010.

Publisher's Note Springer Nature remains neutral with regard to jurisdictional claims in published maps and institutional affiliations.